Solid State Phenomena
ISSN: 1662-9779, Vol. 393, pp 71-77
doi:10.4028/p-9UOfEY

Submitted: 2025-09-27
Revised: 2025-12-10
Accepted: 2026-02-23
Online: 2026-05-18

Remote Epitaxy of SiC: Feasibility, Challenges, and Pathways

Misagh Ghezellou[1,a*], Justinas Palisaitis[1,b], and Jawad Ul-Hassan[1,c]

Department of Physics, Chemistry, and Biology (IFM), Linköping University, SE-58 183, Sweden

[a]Misagh.Ghezellou@liu.se, [b]Justinas.Palisaitis@liu.se, [c]Jawad.Ul-Hassan@liu.se

Keywords: Remote Epitaxy, CVD, Graphene

Abstract. Silicon carbide (SiC) is a promising wide-bandgap semiconductor for advanced quantum technologies. Yet, despite progress in bulk and epitaxial growth, a reliable SiC-on-insulator platform remains lacking. Remote epitaxy, mediated by a 2D interlayer, offers a potential pathway to transferable SiC thin films and substrate reuse. In this work, we examine remote epitaxial growth of SiC on epitaxial graphene. We first evaluate the stability of graphene under SiC growth conditions and find that it degrades significantly at the required high temperatures, primarily due to hydrogen and silane etching. With the conditions yielding the highest-quality SiC epitaxial layer; graphene migrates above the SiC rather than remaining at the interface, demonstrating that true remote epitaxy is not achieved. These results highlight the fundamental challenges of SiC remote epitaxy on graphene and point toward critical directions for future exploration.

Introduction

Silicon carbide (SiC) is a wide band-gap semiconductor with exceptional properties, making it a key material for demanding applications in high-power electronics, optoelectronics, and quantum technologies. [1, 2, 3, 4] In the quantum realm, SiC hosts optically addressable spin qubits, known as color centers, positioning it as a leading platform for integrated quantum photonics. [5, 6, 7] However, realizing this potential requires a scalable SiC-on-insulator platform. Traditional fabrication methods like mechanical polishing and etching struggle to produce the necessary ultra-thin layers at scale. A promising alternative is remote epitaxy, which uses a 2D intermediary layer to grow high-quality, transferable films, also allowing for the cost-saving reuse of expensive SiC substrates. [8, 9, 10]

The growth of an epitaxial film over a 2D intermediary can proceed through three distinct mechanisms. [11, 12, 13] In remote epitaxy, the substrate's electrostatic potential penetrates the 2D layer, guiding the formation of a single-crystalline film that copies the substrate's template. Conversely, quasi-van der Waals epitaxy relies on weak interactions with the 2D layer itself, where the substrate's potential is negligible. Finally, pinhole-based epitaxy occurs when defects in the 2D layer expose the underlying substrate, creating seeding points for direct growth and subsequent lateral overgrowth to form a continuous film. [9]

However, remote epitaxy of SiC faces a unique and critical challenge: polytype control. SiC exists in over 250 polytypes, and replicating a specific one during epitaxy requires step-flow growth on precisely off-cut substrates. [14] Consequently, the intermediary 2D layer must be compatible with this off-cut geometry. Graphene is an ideal candidate as it can be grown epitaxially on SiC. In contrast, materials like hBN, successful for III-V remote epitaxy, are unsuitable for SiC due to their polarity, which disrupts polytype replication. [15] This leads to a significant roadblock: while the epitaxial growth of graphene on SiC is a well-established process, it is typically optimized for on-axis substrates to achieve high uniformity. Research on producing high-quality epitaxial graphene on the required off-axis SiC substrates remains limited, hindering the advancement of SiC remote epitaxy. [16]

In this study, we address this central challenge by investigating the intricacies of SiC remote epitaxy. We explore the growth of epitaxial graphene on off-axis SiC substrates and develop process modifications to overcome the existing obstacles, thereby establishing a pathway for the subsequent remote epitaxial growth of SiC.

Table 1: Growth parameters of different samples grown under solely Ar ambient together with corresponding sample IDs.

Sample ID	Growth Temperature [°C]	SiH_4 flow [ml/min]	C/Si	Growth time [min]
A	1660	11.5	1.2	10
B	1660	3.5	1.2	10
C	1590	5	1.2	1
D	1590	5	1.2	10
E	1590	5	1.2	30
F	1540	5	1.2	30
G	1590	5	1.6	30
H	1590	5	2	30
I	1610	2	2	30

Experimental

All epitaxial layers in this study (graphene and SiC) were grown in a horizontal hot-wall chemical vapor deposition (CVD) reactor with induction heating. Standard highly doped n-type 4°-off 4H-SiC substrates (Si- and C-face) were cut from the same commercial wafer and subjected to RCA cleaning prior to the growth. Carrier gases included Ar, H_2, or their mixtures, with SiH_4 and C_3H_8 serving as Si and C source gases, respectively. Unlike conventional graphite susceptor used for graphene growth, all epitaxial graphene layers were grown on a TaC-coated susceptor, identical to that used for SiC growth.

Graphene was synthesized by the sublimation method. Substrates underwent in-situ surface preparation at 1450 °C for 10 min in H_2, followed by chamber evacuation and introduction of Ar at 200 mbar. The temperature was then raised to 1660 °C, and graphene growth proceeded for 30 min under Ar. To assess graphene preservation under SiC epitaxial growth condition, samples were subsequently exposed to H_2, Ar+SiH_4, and Ar+C_3H_8 ambient at various temperatures.

For SiC-on-graphene growth, Ar was selected as the carrier gas, and the temperature was varied between 1540 °C and 1660 °C. Growth runs were systematically performed with controlled parameter variations to examine their impact on SiC quality and graphene preservation. SiC deposition followed immediately after graphene growth by introducing source gases after pressure adjustment. Detailed parameters and sample IDs are provided in Table 1.

Surface morphology was examined by optical microscopy in differential interference contrast (DIC) mode. Raman spectroscopy was employed to verify graphene presence, assess its quality, and confirm SiC polytype replication. Transmission electron microscopy (TEM) was further used to confirm graphene retention and characterize the interfaces.

Results and Discussion

On the Si-face, epitaxial graphene growth followed a layer-by-layer mode. Fig. 1(a,b) shows optical and Raman data from a 4°-off Si-face substrate, with the Lorentzian fit of the 2D peak (FWHM = 49 cm^{-1}) confirming monolayer graphene above a buffer layer. [17, 18] Cross-sectional HRTEM (Fig. 1(c)) corroborates this structure.

The growth kinetics were examined by extending growth durations (Fig. 1(d)). Beyond 90 min, the 2D FWHM rapidly increased and saturated at $\sim$80 cm^{-1}, indicative of multilayer graphene. This saturation is likely influenced by the TaC-coated susceptor used for SiC growth, which contributes a positive Si partial pressure that suppresses further graphene sublimation.

In contrast, growth on the C-face produced highly non-uniform graphene coverage (Fig. 2). Optical and Raman analyses revealed bare regions without graphene (region A) and multilayer graphene

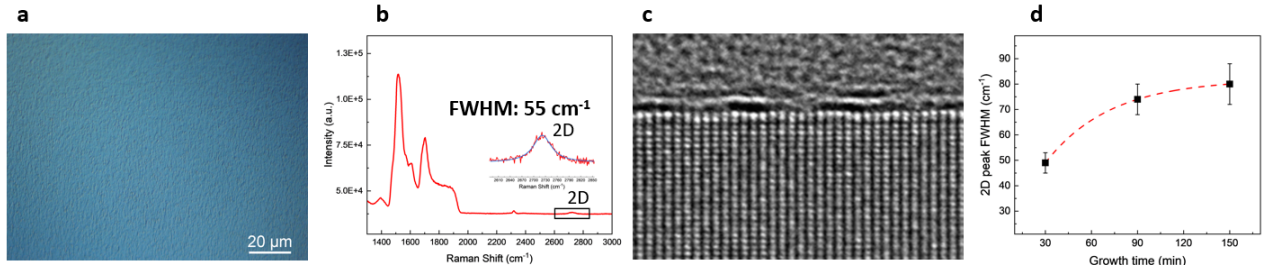

Fig. 1: (a) Optical image showing the surface of a 4°-off Si-face substrate after graphene growth. (b) Raman spectrum illustrating the 2D peak with Lorentzian fit, yielding a FWHM of 49 cm^{-1}. (c) Cross-sectional HRTEM confirming the buffer layer and monolayer graphene. (d) Graph showing the evolution of the 2D peak FWHM with growth time on Si-face substrates.

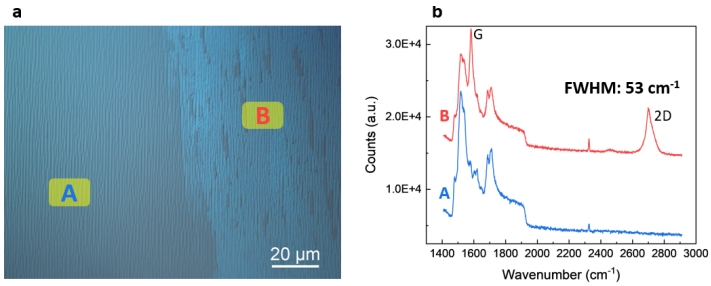

Fig. 2: (a) Optical image showing epitaxial graphene grown on a C-face 4H-SiC substrate with randomly distributed graphene grains. (b) Raman spectra comparing two regions: one without graphene (A) and one with graphene (B).

regions (region B, FWHM = 53 cm^{-1}). These observations agree with reports of turbostratic and uncontrolled graphene formation on the C-face, linked to its lower surface energy. [16]

The stability of epitaxial graphene under SiC growth conditions was tested in different ambient (Fig. 3). Graphene degraded in H_2 above 1300 °C and was fully etched by introducing small flow of SiH_4 in Ar ambient at 1590 °C, while repeating the experiment with C_3H_8 left graphene intact. These results establish SiH_4 as the critical factor driving graphene loss during SiC growth.

SiC growth was next attempted on substrates with epitaxial graphene. At high precursor flow rates (samples A and B, Fig. 4(a,b)), parasitic graphitic deposits formed alongside preserved graphene in step-bunched regions. At reduced flow rates (Fig. 4(c,d)), deposits were suppressed but graphene was etched, indicating a delicate balance between precursor supply and graphene survival.

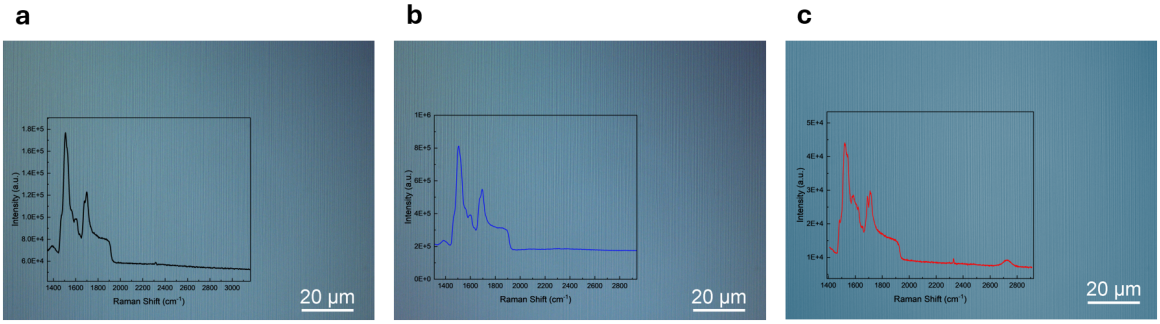

Fig. 3: Optical images and Raman spectra showing graphene layers exposed to (a) H_2 at 1300 °C, (b) Ar+SiH_4 at 1590 °C, and (c) Ar+C_3H_8 at 1590 °C. Raman analysis indicates graphene removal in (a) and (b), while preservation is observed in (c).

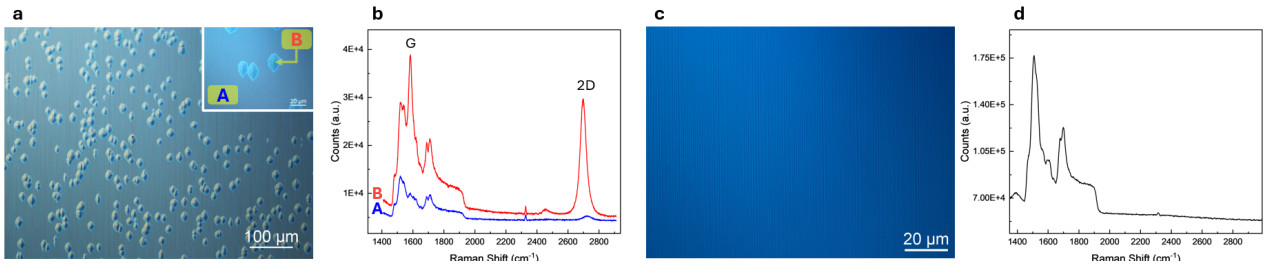

Fig. 4: (a) Optical image showing the surface of sample A, with inset providing higher magnification. (b) Raman spectra from two regions marked in (a). (c) Optical image of sample B. (d) Raman spectra from the region marked in (c).

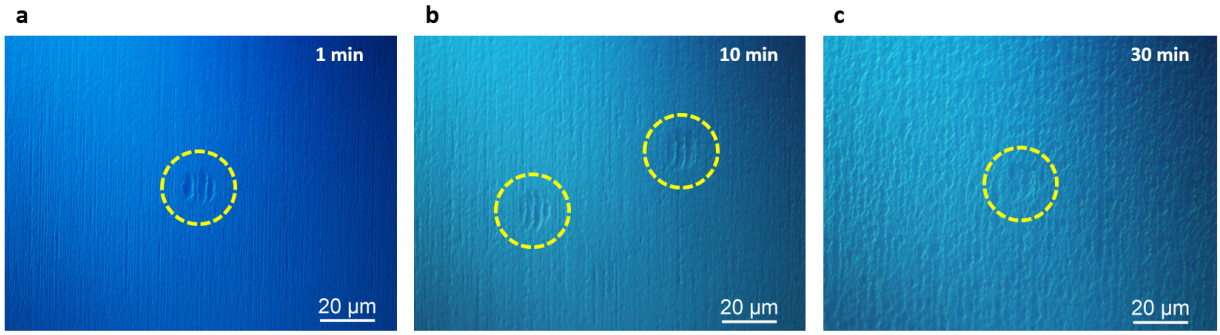

Fig. 5: Optical images showing the surfaces of (a) sample C, (b) sample D, and (c) sample E after SiC growth for 1, 10, and 30 minutes, respectively. Surface pits linked to Si droplets are highlighted by yellow dashed circles.

Lowering the temperature to 1590 °C (C/Si = 1.2) enabled SiC nucleation followed by epitaxial growth at a rate of ∼1.3 μm/h, but Raman spectra showed no graphene peaks (Fig. 5). With increasing growth time, Si-droplet-related pits diminished and zigzag step structures characteristic of SiC emerged, yet graphene loss remained unavoidable.

To mitigate this, higher C/Si ratios (1.6 and 2.0) were explored (Fig. 6). Graphene-related peaks reappeared in Raman spectra, but surface quality degraded, with defective graphene or graphite features forming. Thus, higher C/Si ratios favor graphene preservation but compromise film morphology.

Optimized conditions were achieved in sample I, grown at 1610 °C, C/Si = 2.0, and reduced SiH_4 flow (2 ml/min). No droplet pits were observed (Fig. 7(a)), triangular defects indicated SiC growth, and Raman spectra revealed 1–2 graphene monolayers (Fig. 7(b)). TEM confirmed 4H-SiC stacking (Fig. 7(c–f)). However, the graphene signal originated from the surface of the SiC film rather than the buried interface, ruling out true remote epitaxy.

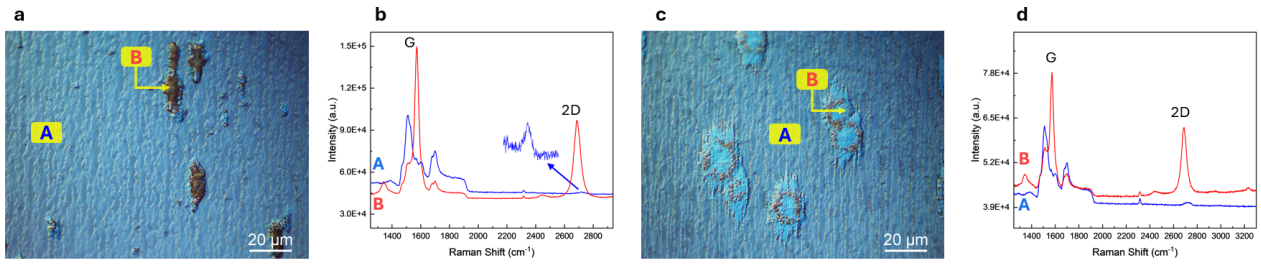

Fig. 6: (a, c) Optical images showing SiC grown on epitaxial graphene with different C/Si ratios: (a) sample G (C/Si = 1.6) and (c) sample H (C/Si = 2.0). (b, d) Raman spectra from the regions marked in (a) and (c), respectively.

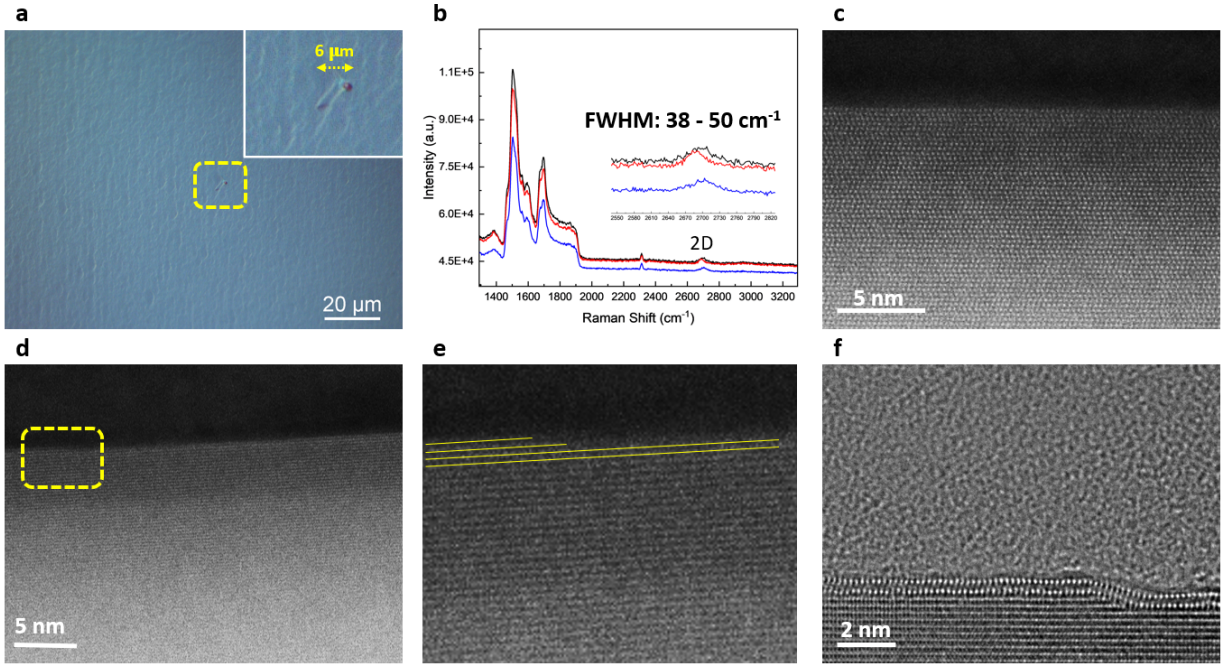

Fig. 7: (a) Optical image showing the surface of sample *I* with a triangular defect characteristic of SiC growth. (b) Raman spectrum indicating the presence of 1–2 graphene monolayers. (c) TEM image confirming the 4H polytype of the epitaxial SiC layer. (d, e) TEM images showing step edges on the surface of sample *I*. (f) HRTEM image revealing a monolayer graphene above a buffer layer.

Two scenarios were considered: (i) graphene was etched during SiC growth and reformed upon cooling, or (ii) Si and C atoms penetrated beneath graphene to nucleate SiC, as reported for quasi-2D GaN. [19] Additional experiments supported the first scenario. Suppressing graphene formation by raising chamber pressure after growth or introducing small H_2 flows eliminated Raman graphene peaks, confirming that the observed graphene formed during cooldown rather than surviving growth.

Finally, the effect of H_2 addition was examined. At very low H_2/Ar (0.013), surfaces resembled step-bunched graphene (Fig. 8(a)), while higher H_2/Ar (0.25) enabled SiC growth with smoother step edges (Fig. 8(b)). Yet in both cases, Raman showed no graphene, indicating that hydrogen promotes SiC growth but accelerates graphene loss.

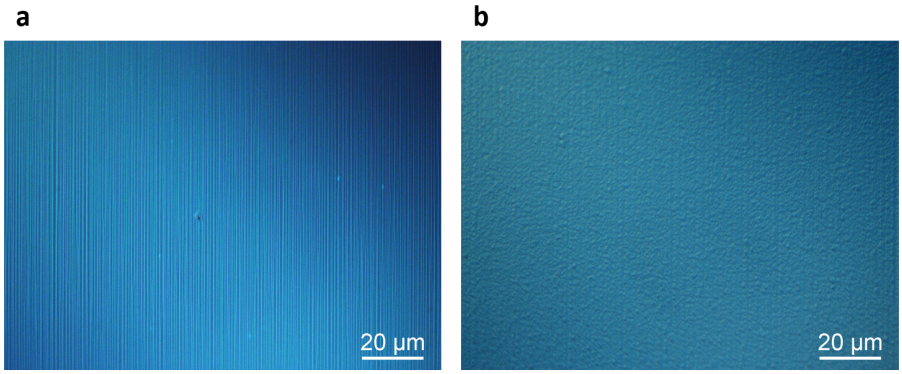

Fig. 8: Optical images showing sample surfaces after SiC growth with added H_2 at H_2/Ar ratios of (a) 0.013 and (b) 0.25.

Summary

This study examined the feasibility of remote epitaxy of SiC using graphene as an intermediary layer. Preserving graphene during SiC growth proved highly challenging: it was consistently etched at high temperatures, low C/Si ratios, or in hydrogen- and silane-containing ambients. Even under conditions resulting in high quality SiC epitaxial layers, Raman and TEM analyses showed that graphene reformed only during cooldown, rather than surviving beneath the SiC epitaxial layer.

Overcoming these limitations will require lowering effective growth temperatures through improved precursor chemistry or ambient control, and exploring alternative substrate orientations that support island nucleation instead of step-flow growth. Addressing issues such as graphene-induced terrace widening, which promotes 3C-SiC nucleation, will also be critical.

Acknowledgments

The Swedish Research Council (VR) grant No.2020-05444 and European Union's Horizon Europe research and innovation program grant for the project SPINUS (Grant No. 101135699) are acknowledged for financial support. Swedish Research Council and the Swedish Foundation for Strategic Research are acknowledged for access to ARTEMI, the Swedish National Infrastructure in Advanced Electron Microscopy (2021-00171 and RIF21-0026).

References

[1] T. Kimoto and Y. Yonezawa, "Current status and perspectives of ultrahigh-voltage sic power devices," *Materials Science in Semiconductor Processing*, vol. 78, pp. 43–56, 2018.

[2] H. Tsuchida, I. Kamata, T. Miyazawa, M. Ito, X. Zhang, and M. Nagano, "Recent advances in 4h-sic epitaxy for high-voltage power devices," *Materials Science in Semiconductor Processing*, vol. 78, pp. 2–12, 2018.

[3] F. La Via, D. Alquier, F. Giannazzo, T. Kimoto, P. Neudeck, H. Ou, A. Roncaglia, S. E. Saddow, and S. Tudisco, "Emerging sic applications beyond power electronic devices," *Micromachines*, vol. 14, no. 6, p. 1200, 2023.

[4] M. Buffolo, D. Favero, A. Marcuzzi, C. De Santi, G. Meneghesso, E. Zanoni, and M. Meneghini, "Review and outlook on gan and sic power devices: industrial state-of-the-art, applications, and perspectives," *IEEE Transactions on Electron Devices*, 2024.

[5] D. M. Lukin, M. A. Guidry, J. Yang, M. Ghezellou, S. Deb Mishra, H. Abe, T. Ohshima, J. Ul-Hassan, and J. Vučković, "Two-emitter multimode cavity quantum electrodynamics in thin-film silicon carbide photonics," *Physical Review X*, vol. 13, no. 1, p. 011005, 2023.

[6] D. J. Christle, A. L. Falk, P. Andrich, P. V. Klimov, J. U. Hassan, N. T. Son, E. Janzén, T. Ohshima, and D. D. Awschalom, "Isolated electron spins in silicon carbide with millisecond coherence times," *Nature materials*, vol. 14, no. 2, pp. 160–163, 2015.

[7] T. Bosma, J. Hendriks, M. Ghezellou, N. T. Son, J. Ul-Hassan, and C. H. van der Wal, "Broadband single-mode planar waveguides in monolithic 4h-sic," *Journal of Applied Physics*, vol. 131, no. 2, p. 025703, 2022.

[8] H. Kim, C. S. Chang, S. Lee, J. Jiang, J. Jeong, M. Park, Y. Meng, J. Ji, Y. Kwon, X. Sun *et al.*, "Remote epitaxy," *Nature Reviews Methods Primers*, vol. 2, no. 1, p. 40, 2022.

[9] C. S. Chang, K. S. Kim, B.-I. Park, J. Choi, H. Kim, J. Jeong, M. Barone, N. Parker, S. Lee, X. Zhang *et al.*, "Remote epitaxial interaction through graphene," *Science Advances*, vol. 9, no. 42, p. eadj5379, 2023.

[10] H.-J. S. Roland Rupp, Guenther Ruhl, "Semiconductor device and a method for forming a semiconductor device," *U. S. Patent No. 20170018614A1*, 25 Dec 2018.

[11] Y. Kim, S. S. Cruz, K. Lee, B. O. Alawode, C. Choi, Y. Song, J. M. Johnson, C. Heidelberger, W. Kong, S. Choi *et al.*, "Remote epitaxy through graphene enables two-dimensional material-based layer transfer," *Nature*, vol. 544, no. 7650, pp. 340–343, 2017.

[12] K. Chung, C.-H. Lee, and G.-C. Yi, "Transferable gan layers grown on zno-coated graphene layers for optoelectronic devices," *Science*, vol. 330, no. 6004, pp. 655–657, 2010.

[13] S. Manzo, P. J. Strohbeen, Z. H. Lim, V. Saraswat, D. Du, S. Xu, N. Pokharel, L. J. Mawst, M. S. Arnold, and J. K. Kawasaki, "Pinhole-seeded lateral epitaxy and exfoliation of gasb films on graphene-terminated surfaces," *Nature communications*, vol. 13, no. 1, p. 4014, 2022.

[14] T. Ueda, H. Nishino, and H. Matsunami, "Crystal growth of sic by step-controlled epitaxy," *Journal of Crystal Growth*, vol. 104, no. 3, pp. 695–700, 1990.

[15] X. Wang, J. Choi, J. Yoo, and Y. J. Hong, "Unveiling the mechanism of remote epitaxy of crystalline semiconductors on 2d materials-coated substrates," *Nano Convergence*, vol. 10, no. 1, p. 40, Aug 2023.

[16] G. R. Yazdi, T. Iakimov, and R. Yakimova, "Epitaxial graphene on sic: a review of growth and characterization," *Crystals*, vol. 6, no. 5, p. 53, 2016.

[17] A. C. Ferrari, J. C. Meyer, V. Scardaci, C. Casiraghi, M. Lazzeri, F. Mauri, S. Piscanec, D. Jiang, K. S. Novoselov, S. Roth *et al.*, "Raman spectrum of graphene and graphene layers," *Physical review letters*, vol. 97, no. 18, p. 187401, 2006.

[18] R. Yakimova, C. Virojanadara, D. Gogova, M. Syväjärvi, D. Siche, K. Larsson, and L. I. Johansson, "Analysis of the formation conditions for large area epitaxial graphene on sic substrates," in *Materials Science Forum*, vol. 645. Trans Tech Publ, 2010, pp. 565–568.

[19] Z. Y. Al Balushi, K. Wang, R. K. Ghosh, R. A. Vilá, S. M. Eichfeld, J. D. Caldwell, X. Qin, Y.-C. Lin, P. A. DeSario, G. Stone *et al.*, "Two-dimensional gallium nitride realized via graphene encapsulation," *Nature materials*, vol. 15, no. 11, pp. 1166–1171, 2016.